Available online at www.sciencedirect.com
SCIENCE DIRECT®
Polymer 44 (2003) 5387–5396
polymer
www.elsevier.com/locate/polymer

Structure and properties of polyamide 6 and 4-aminomethylcyclohexane carboxylic acid copolymers with an unusually short helical pitch for nylons

N.S. Murthy[a,*], R.G. Bray[b]

[a]*Department of Physics, University of Vermont, Burlington, VT 05405, USA*
[b]*Honeywell International, Specialty Materials, Morristown, NJ 07962, USA*

Received 30 January 2003; received in revised form 16 May 2003; accepted 21 May 2003

Abstract

Segments of 4-aminomethylcyclohexane carboxylic acid (AMCC) inserted into the polyamide 6 (nylon 6, N6) chain are distributed in both the crystalline lattice and the amorphous regions. Thermal, spectroscopic and X-ray diffraction data indicate that the N6/AMCC copolymer crystallizes in an otherwise thermodynamically unfavorable γ crystalline form of N6. The chain-axis repeat or the helical pitch of 15.7 Å of this copolymer is the shortest ever reported for N6. This is accompanied by an expansion of the lattice in the equatorial plane. This short pitch was observed at comonomer concentrations as low as 10 mol%, and the lattice remains otherwise essentially same as that of N6 up to about 30 mol% AMCC. Conformational constraints imposed by interchain hydrogen bonding between N6 and AMCC with chain-axis repeat distance of 17.2 and 15.8 Å, respectively, are thought to be the reason for this shortened helical pitch. This short pitch (length scale ~10 Å) results in a lower chain-modulus. Differences in the H-bond strength are invoked to explain the higher glass transition temperature in the dry copolymer, i.e. the increased stiffness of the multiple chain segments (length scales >10 Å) and the differing response to guest molecules such as water. Although the mechanical properties (tensile strength, shrinkage and creep) of the dry copolymer and the homopolymer were similar, moisture had a dramatically different effect on the two polymers. This behavior is attributed to the differences in lamellar morphology (length scales ~100 Å), especially the contribution of the amorphous regions, which determine the bulk properties.

Keywords: Copolymers; Structure; Nylons

1. Introduction

Copolymers in which comonomer units are inserted into the main chain of a host polymer provide a robust and economical route to enhance the performance range of a polymer. The comonomer units in crystallizable polymers are typically not incorporated into the same crystal lattice. For instance, even though the two comonomers in nylon 6/nylon 6,6 (N6/N66) copolymers are quite similar, the resulting copolymer forms a eutectic, and the two units tend to crystallize into different domains [1]. Often, the chain segments containing the co-units are segregated into the amorphous regions, and aging/annealing may cause further phase separation into domains of segments with and without the comonomer units [2]. Against this background, it is useful to investigate in detail polymers in which the co-units are distributed in both the crystalline and amorphous regions and are in thermodynamic equilibrium. This class of copolymers can be obtained from isomorphous polymer pairs [3]. Since polymers are prone to adopt different structures, isomorphism is defined as statistical distribution of different units within the same crystallite, without insisting that the crystal lattice remain unchanged after substitution, as required by the crystallographic definition of isomorphous replacement [4]. A subclass of such polymers is one in which the two homopolymers have different crystal structures. In this instance, structure of the copolymer abruptly changes from one type to another at a certain composition, and both the homopolymer structures may also be simultaneously present at intermediate compositions [5]. We study here one such copolymer of N6 with 4-aminomethylcycohexane carboxylic acid (AMCC, Fig. 1), here after referred to as the copolymer.

* Corresponding author. Tel.: +1-802-656-0308; fax: +1-802-656-0817.
E-mail address: sanjeeva.murthy@uvm.edu (N.S. Murthy).

0032-3861/03/$ - see front matter © 2003 Elsevier Ltd. All rights reserved.
doi:10.1016/S0032-3861(03)00465-8

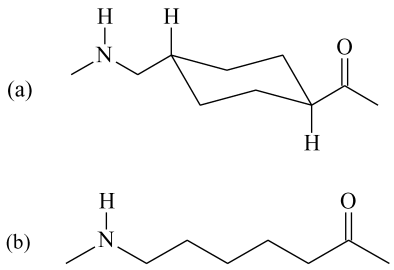

Fig. 1. Chemical structure of (a) AMCC and (b) nylon 6.

The first report on the N6/AMCC copolymer suggested that AMCC and the N6 monomers were interchangeable in the crystal lattice [6]. This assertion was disputed in a later study that interpreted the X-ray diffraction (XRD) data as indicating cocrystallization rather than isomorphous replacement of AMCC in the N6 lattice [7]. The term cocrystallization was used to suggest dissolution of AMCC residues inside the N6 lattice, and not to the formation of two side-by-side crystalline phases as in a eutectic. It was argued that the AMCC segments are present as defects in the N6 lattice, which is left unchanged, and thus reducing the crystalline order. We here present X-ray diffraction, spectroscopic and thermal data from highly drawn fibers of these copolymers which show that although the crystalline lattice of the copolymer is similar that of the host lattice (N6), the incorporation of AMCC into the N6 lattice considerably decreases the chain-axis repeat distance and increases the lateral unit-cell dimensions.

Nylons crystallize in two crystalline forms that are commonly referred to as α and γ. The α is stable in nylons below and up to nylon 4, and the γ is stable in nylon 8 and above. Nylon 6 is unique in that it crystallizes easily in either of the crystalline forms, and readily transforms from one to another [8]. The hydrogen bonds are between antiparallel chains in the α form and between parallel chains in the γ form. Both the unit cells are monoclinic; α form: $a = 9.56$ Å, b (fiber axis) $= 17.24$ Å, $c = 8.01$ Å, $\beta = 67.5°$; γ form: $a = 9.33$ Å, b (fiber axis) $= 16.88$ Å, $c = 4.78$ Å, $\beta = 121°$. The hydrogen bonds are along the a-axis in the α form and along the c-axis in the γ form. The important difference between the two structures that is relevant for this paper is that the chain-axis repeat is 17.24 Å in the α form due to its extended planar conformation, and is 16.88 Å in the γ form due to its twisted helical conformation. A third crystalline phase, which is often considered to be a variants of γ, is the β form in which the chains have disordered conformation with no definite chirality; the chain-axis repeat of this phase is about the same as that of γ (16.7 Å) [9]. Other metastable and psuedohexagonal phases have also been postulated for N6. In these phases the lateral packing of the chains is such that a single interchain separation of ~4.1 Å is observed [10,11]. But these metastable phases are more likely even more disordered variants of the γ form than the β form [8,12]. The α- and γ-N6 are easily identified by their distinct X-ray diffraction patterns. Here we study γ crystalline form of N6 obtained as a result of random insertion of AMCC into the N6 chain.

2. Materials and methods

A bench-scale reactor was charged with caprolactam, 5–25 mol% *trans*-4-(aminomethyl) cyclohexanecarboxylic acid and 0–10 wt% water. The contents were purged continuously with inert gas and heated at 250 °C with stirring for 2–4 h. The copolymer mass was then annealed at 140 °C for several hours, milled after embrittling at low temperature, leached with boiling water to remove 6–9 wt% monomer and dried in vacuo at 115 °C. The concentrations quoted in the text are the feed ratios. Since more of the caprolactam part of the crude copolymer is removed by leaching, the apparent mole fraction of comonomer in leached polymer is slightly higher than in the reactor charge. For instance, a 17 nominal mol% values given in the text corresponds to 18.4 mol% of AMCC in the final product.

Most significant structural data reported here were obtained from spun and drawn fibers with 17 mol% AMCC. N6 and a copolymer of about the same molecular weight (55 FAV, formic acid viscosity—the relative viscosity of an 11% solution of nylon in formic acid) [13] were spun under the normal conditions, drawn 3.2 times, and heat set in an autoclave at 132 °C. Films of 125 μm thickness cast with this 17 mol% AMCC resin, films cast with a 10 mol% AMCC (90 FAV) resin, and injection-molded plaques with 17 mol% AMCC (80 FAV) resin were also investigated.

X-ray diffraction data (XRD) were obtained from uniaxially drawn fibers, unoriented films and injection molded plaques. 2D diffraction data were obtained on a Bruker AXS detector using Cu Kα radiation from a sealed tube. Franks' mirrors and Ni filters were used to collimate and filter the primary beam. Sample to detector distance was 6.5 cm. 1D data, equatorial and meridional scans (perpendicular and parallel to the fiber axis, respectively) and fast-rotational scans (rotational averaged data for crystallinity determination), were collected on a Philips diffractometer (PW3700) in θ/2θ mode with Cu Kα radiation in transmission geometry. For these 1D scans, the fibers were wound on a 1 cm × 1 cm rectangular frame. For fast-rotational scans, this sample frame was spun at a rapid rate (60 rev min^{-1}) in its own plane while the detector was stepped at a slow rate (10 s per 0.1° step) [14,15]. Data from cast films were obtained in parafocus geometry on another Philips diffractometer. IR spectra were obtained on a Nicolet Magna 550 spectrometer/SpectraTech IR PLAN microscope using a single-filament of the drawn fiber. DSC scans and mechanical test data were obtained using standard methods and equipment. Creep measurements were carried out using a setup that permitted long-term observation at various levels of humidity.

The crystallinities were determined from the ratio of the area under the crystalline peaks to the total scattered intensities using the data from $2\theta = 5-35°$. These areas were obtained by least squares fitting the crystalline peaks and an amorphous halo to the observed data [14]. Scans obtained in parafocus geometry were used for unoriented samples, and 'fast-rotational' scans were used for fibers. Crystallite sizes were determined using the Scherrer equation [16]. Modified Lorentzian peak shape approximation with a measured instrumental broadening 0.1° was used for parafocus scans from unoriented samples, and Gaussian peak shape approximation with a measured instrumental broadening of 0.2° used for transmission scans from oriented fibers.

3. Results

For comparison, the key thermal parameters for the two homopolymers are listed in Table 1. Some of the thermal analysis data obtained from DSC scans of N6 and the copolymer are listed in Table 2. The glass transition temperature (T_g), crystallization temperature during heating (Tch) and the melting point (T_m) all appeared to increase linearly with the comonomer content from the lowest AMCC composition (5%) used in this study (Fig. 2). The melting point of 355 °C at 50% AMCC is much higher than 260 °C predicted by linear extrapolation of the data up to 30% AMCC (30 and 50% data from literature [7]). But, it should be noted that 50% sample could contain AMCC-rich fractions because of synthesis problems such as undesirable premature crystallization of the copolymer; the AMCC comonomer does not fully dissolve if the viscosity increases and remelting/transamidation does not occur.

Preliminary investigation of the crystallization temperature during cooling (T_{cc}), which is a very sensitive indicator of the crystallization kinetics, suggested that at typical cooling rates of 10–20 °C/min, T_{cc} of the copolymer is about the same as in N6 (178–182 °C). However, T_{cc} measured at a wider range of cooling rates showed copolymer to be different from that of N6 (Fig. 3). Just like any other polymer, the copolymer crystallized at lower temperature when the melt is cooled at a faster rate. But, at every cooling rate, the copolymer crystallized at a higher temperature than N6. As will be discussed later, this is indicative of the different structures into which the copolymer and the homopolymer crystallize.

Table 1
Thermal properties of the nylon 6 and AMCC homopolymers

Thermal properties	N6	AMCC[7]
T_g (°C)	43	192
T_m (°C)	214 (γ); 222 (alpha)	410
T_{ch} (°C)	60	240–250

T_m is the melting temperature. T_g is glass transition temperature; T_{ch} is the crystallization temperature upon heating.

Table 2
Some thermal and mechanical properties of the copolymer and nylon 6 (AMCC (mol%): pellets, 15–17; fibers, 17 and films, 10)

	N6		Copolymer	
	Dry	Wet	Dry	Wet
Thermal properties				
T_m (°C) pellets	214 (γ)		227	
In water		155		132
T_g (°C) pellets	43		66	
Textured yarn 50% RH		−9		4
T_{ch} (°C) pellets	60		98	
Fiber properties				
4.5 drawn: breaking elongation (%)	21		19	
Tenacity (g/den)	5.7		5.2	
Modulus (g/den)	33		34	
Shrinkage (%), drawn yarn: at 177 °C	11.2		9.9	
In boiling water		12.7		21.6
Shrinkage (%), HS/relaxed yarn: at 177 °C	4.4		3.3	
In boiling water		3.7		10.7
Creep elongation (%)	0.5		0.5	
58% RH		4.3		5.7

T_m, T_g and T_{ch} are melting temperature, glass transition temperature and the temperature of crystallization upon heating, respectively. The conditions of 'wet' measurements are given in the first column.

Some of the mechanical properties are summarized in Table 2. The mechanical properties (Young's modulus, yield stress, yield strain, yield energy, flexural modulus, and flexural stress) in injection molded plaques (not given in the table) of the copolymer were similar to those in the homopolymer. Modulus measured on a 5 mil (125 μm) film was about the same in the copolymer and N6 over a range of humidity (Fig. 4). The plateau modulus of 100 kpsi at high humidity, equivalent to about 7 g/den, and the other values seen in this figure are typical for undrawn N6 fibers. The effect of moisture is consistent with the data in Fig. 5 which shows that water absorption was only marginally higher in the copolymer, and this could be attributed to its lower crystallinity. Break elongation, tenacity and modulus of the N6/AMCC fiber were not significantly different from that of N6 fiber. Dry shrinkage, i.e. the shrinkage measured upon heating the fiber to a predetermined temperature in dry atmosphere, of the copolymer was about the same as in N6: ~10% for the spun–drawn fiber and ~4% for the textured fiber. But, some of these properties changed significantly in the presence of water (51% RH): heat-induced shrinkage was higher in the copolymer than in the homopolymer, e.g. when fibers (5.0× drawn) are immersed in boiling water, the copolymer shrunk by 30% and N6 by 16%; the creep

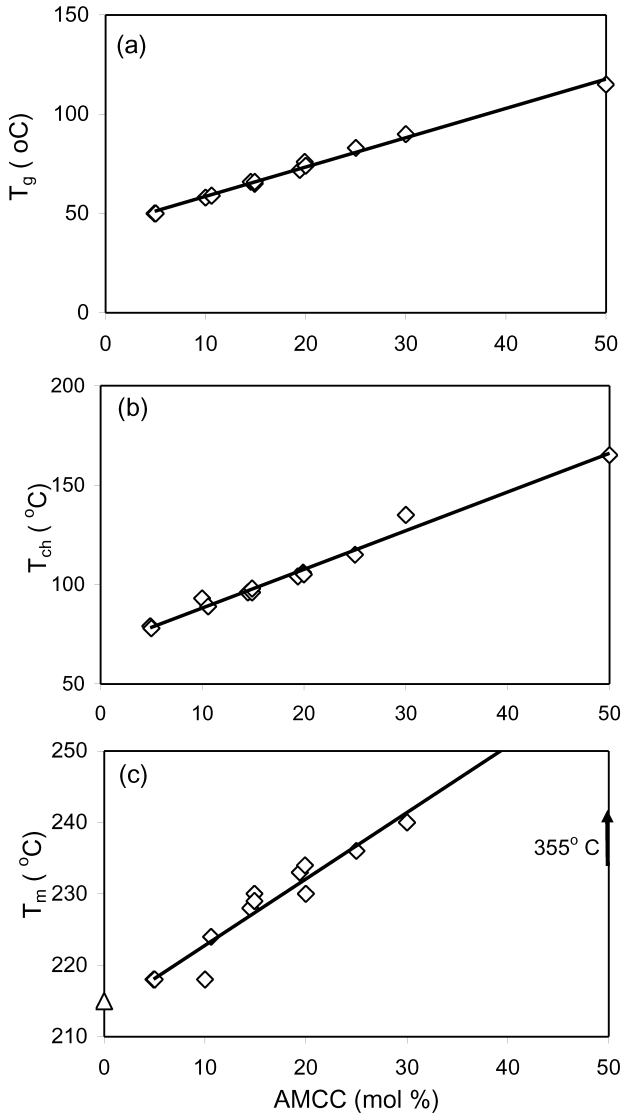

Fig. 2. Changes in the three characteristic temperatures in the copolymer with AMCC concentrations, (a) glass transition temperature T_g; (b) crystallization temperature during heating; (c) melting point T_m; the T_m's for 30 and 50% AMCC are from Ref. [4].

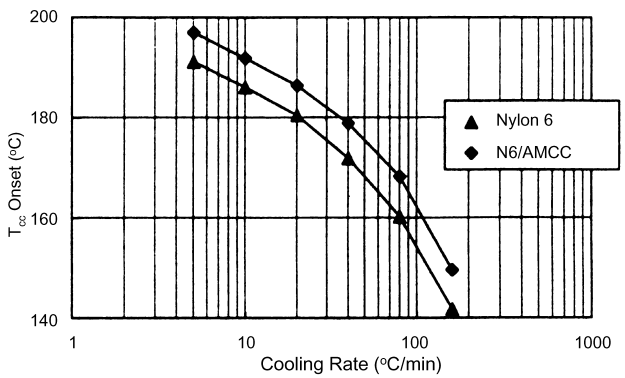

Fig. 3. Comparison of the crystallization temperature during cooling (T_{cc}) of the copolymer and N6 at several cooling rates.

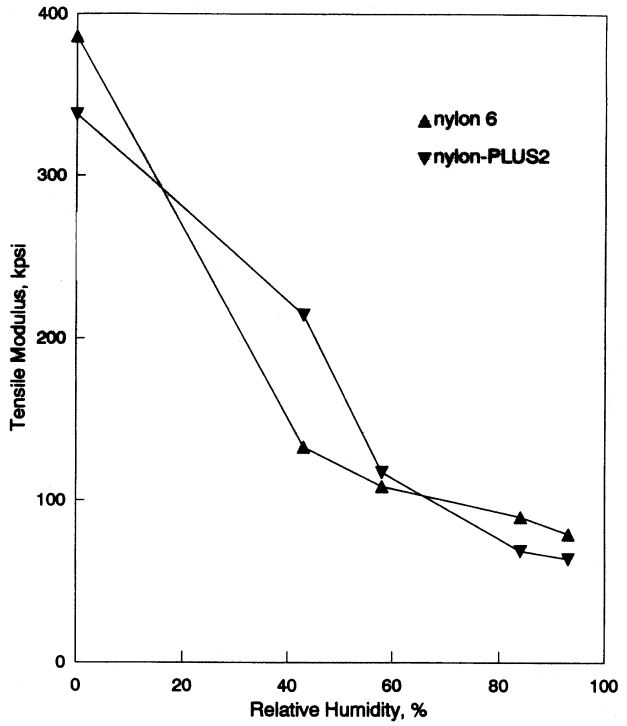

Fig. 4. Decrease in the modulus in 5 mil films of the copolymer (10% AMCC) and N6 with increase in humidity.

data (Fig. 6) also showed that the moisture has a much larger effect in the copolymer than in N6.

Fig. 7 compares the XRD patterns from α-N6, γ-N6 and the copolymer fibers. The α form was from an annealed drawn fiber, and the γ form was from a KI/I_2- treated fiber [17]. These data were obtained with the fiber-axis tilted ~15° with respect to the detector plane so as to catch the higher order meridional reflections. The similarities in the diffraction photographs of the copolymer and γ-N6, allowing for the higher degree of disorder and lower crystallinity in the copolymer, indicate that the copolymer is in the γ crystalline form. But, there is one important difference: the 0 *k* 0 reflections in the copolymer are shifted to higher angles as can be clearly seen in the position of the 0 6 0 reflection. The data thus indicate that

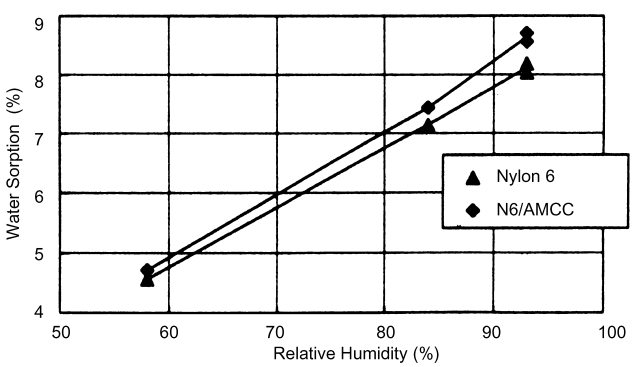

Fig. 5. Water sorption at three levels of humidity in the copolymer (10% AMCC) and N6 films after the films were conditioned by boiling in water overnight.

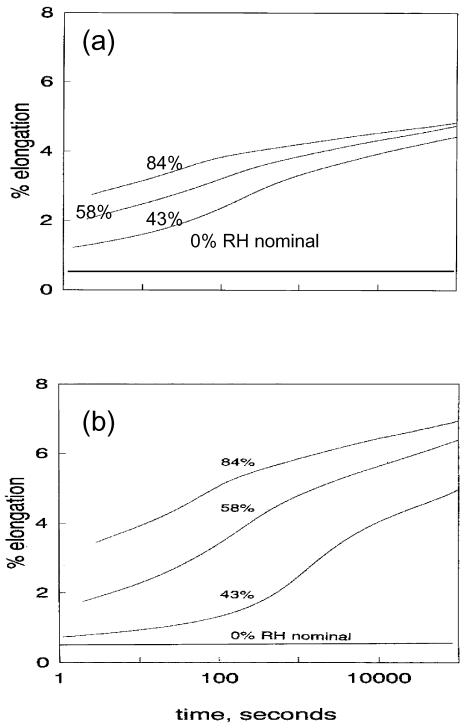

Fig. 6. Comparison of the single-filament creep elongation measured at 30 °C in (a) N6 and (b) the copolymer (17% AMCC).

the chain-packing in the copolymer is similar to that in γ-N6, except that the chain-axis repeat of the copolymer is shorter than that of N6.

Fig. 8a and b shows examples of the equatorial and meridional scans from the homopolymer and the copolymer (17% AMCC) obtained from as-spun (undrawn) fibers. The equatorial scans of the two fibers (Fig. 8a) are quite similar, and indicate γ to be the major crystalline fraction in both the fibers. The only difference is that the peaks are shifted to lower angles indicating a larger unit cell in the equatorial plane. The meridional scans for the two fibers are also quite similar (Fig. 8b), with the exception that the 0 2 0 peak (at ~11°) occurs at a higher-angle in the copolymer than in N6. Because of the low orientation of these as-spun fibers, the intensity distribution at 20° has contribution from both the equatorial and meridional peaks, and hence is not useful. Fig. 8c and d shows examples of the equatorial and meridional scan when these fibers are drawn and annealed. During this process, N6 transforms into α form, but the copolymer remains as γ. The assignments of the 0 *k* 0 reflections in Fig. 8d is unambiguous because the fibers are highly oriented (degree of orientation calculated from the azimuthal width of the equatorial peak is ~0.93), and the scans were obtained so as to minimize the contributions from the off-axes reflections. Most significant is that the meridional 0 *k* 0 reflections in the heat-set copolymer fibers show that the chain-axis repeat in the copolymer is 15.7 Å, which is shorter than that observed in N6: 16.9 in γ form and 17.2 Å in α form.

Crystallinities of the fibers determined from fast-rotation scans (not shown here), which randomize the orientational effects of the polymer chains, are given in Table 3 for some of the fibers used for this study. These crystallinities were calculated using results of profile analysis similar to those shown for unoriented films in Fig. 9. Drawn fibers of the copolymer had lower crystallinity than the homopolymer produced under similar processing conditions. Results from as-cast films support this finding: whereas the crystallinity of an as-cast N6 film increases from 17% to about 34% upon annealing (from a mixture of γ (major) and α (minor) to mostly α), the crystallinity of the copolymer increases from 18 to 26% (γ both before and after annealing). The lower crystallinity of the copolymer was confirmed by the DSC measurements which showed the area under the crystallization peak for the copolymer was only half of that observed for N6 (34 vs. 61 J/g). These values were obtained upon cooling from the melt during which it was also noticed that exotherms for crystallization of the copolymer were narrower than for N6. The narrower peak is attributed to the

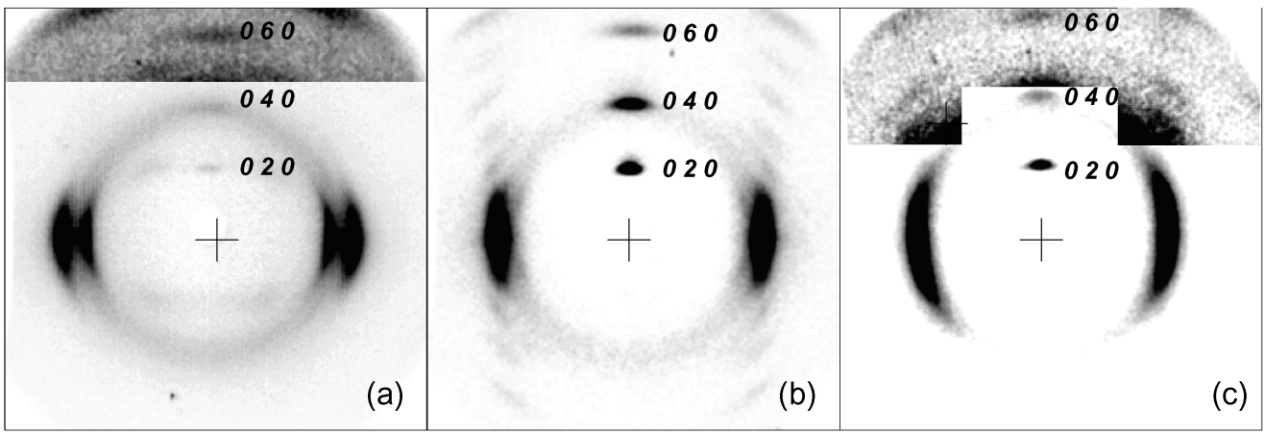

Fig. 7. Fiber X-ray diffraction photograph of (a) α-N6, (b) γ-N6 and (c) the copolymer. The fibers are tilted by 15° towards the detector plane so as to catch the higher-angle meridional reflections. The fiber axis is vertical. The intensity near the 0 6 0 peak in the α fiber and the copolymer pattern have been rescaled to show the weak reflections in this area.

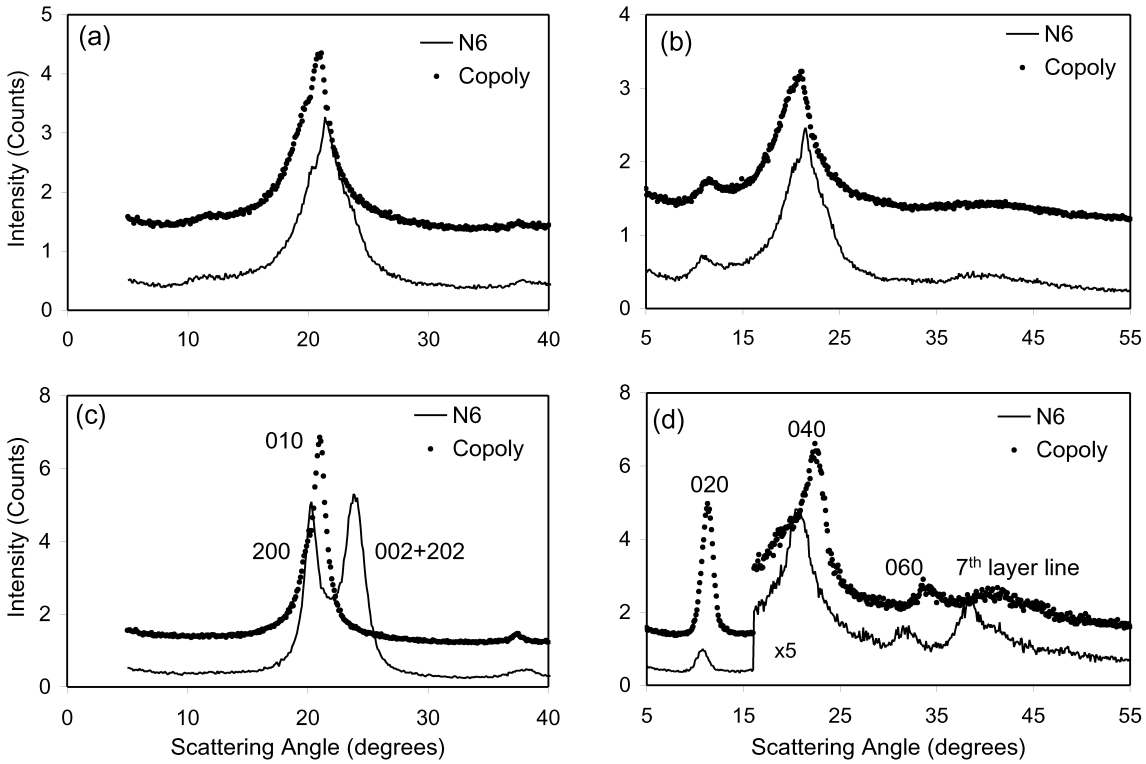

Fig. 8. X-ray diffraction scans from fibers of N6 and the copolymer (17% AMCC). The small circles are from the copolymer and the full lines are for the homopolymer. Undrawn yarns: (a) equatorial and (b) meridional. Drawn and annealed (heat-set) yarns: (c) equatorial and (d) meridional.

formation of a single crystalline polymorph in the copolymer and a mixture of α and γ crystals in N6.

The homopolymer exists either in the α form, a mixture of α and γ crystalline forms, or in the γ form depending on the spin/draw/heat-set conditions. In contrast, the copolymer could be obtained only in the γ form (Figs. 8 and 9a), and retained this form and the short chain-axis repeat even after annealing in an autoclave. These results are different from the previously published XRD data on these copolymers [7]. However, we did find the structures reported earlier by Prince et al. [7] in some of our samples. Scans from an occasional sample (Fig. 9b; 17 mol% AMCC), is similar to the scan from a 70/30 (N6/AMCC) sample in Prince et al. We also observed a third class of patterns upon extended annealing (Fig. 9c). We attribute these results to phase separation induced by crystallization of the α-N6 and the copolymer (copolymer because the meridional peaks is at 11.3° 2θ). The scan from the 50% AMCC polymer is almost identical to that of AMCC homopolymer (Fig. 10). The scans of the type given in Fig. 9b and c, which were observed only rarely in our work and not expected at the comonomer concentrations used here, might be due to the problems similar to those that were alluded to earlier with the synthesis at higher AMCC concentration. AMCC may not be fully incorporated into the polymer chain because of premature crystallization of the copolymer that increases the viscosity and transamidation does not occur.

Table 3
Crystallinity (crystalline index, %) comparison of the N6 and copolymer films and fibers processed under the same conditions

Processing condition	Nylon 6	Copolymer
As-cast film	17	18
As-cast film, boiled overnight in water	34	26
Undrawn fiber	20	9
Normal drawn fiber	25	9
Normal heat-set (annealed) fiber	36	25

The IR spectra (Fig. 11) and Raman spectra (Fig. 12) confirm that the chain-conformation in the copolymer is same as that in the γ crystalline form typically seen in fibers spun at high-speed or treated with iodine. Each spectrum is a composite of the amorphous and the crystalline components (either α or γ phase). The latter typically have sharper peaks, often overlapping the amorphous peaks. The copolymer spectra are very similar to γ-N6 spectra and noticeably different from the α-N6 spectra. This is even more apparent in the polarized IR and Raman spectra. Of specific note are the absence of α-phase peaks at 1476 and 1418 cm^{-1} (Raman and IR), 1309 (Raman) and 933 (IR). The copolymer and γ-N6 show characteristic peaks at 1300/1299 and 922/923 cm^{-1} (Raman).

4. Discussion

4.1. Structure

The data presented here show that the copolymer

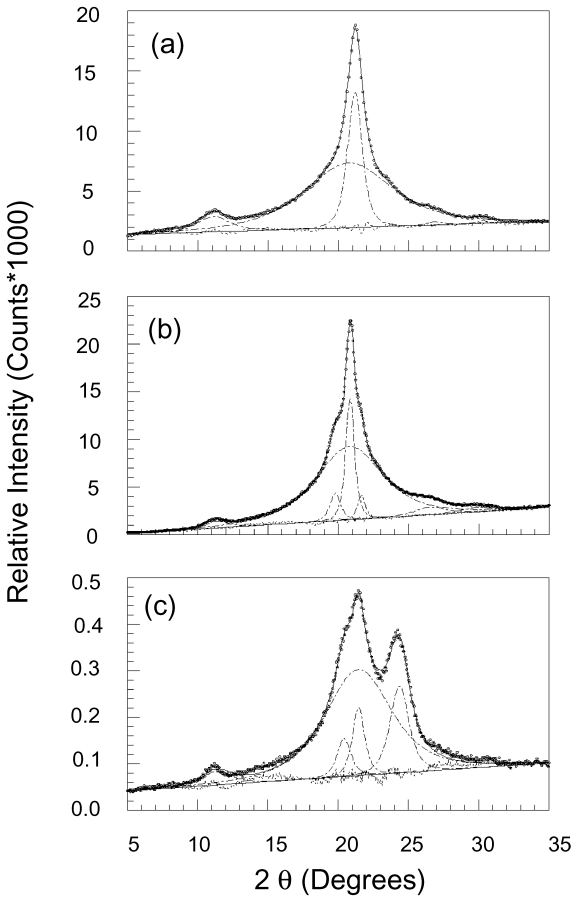

Fig. 9. XRD scans of films from three different preparations. (a) With 10% AMCC and boiled in water. (b) With 17% AMCC and boiled in water. (c) With 10% AMCC and annealed at 120 °C (dry atmosphere). The small circles are the observed data, the peaks shown by the broken lines show how the data can be resolved in to various crystalline (narrow) peaks and an amorphous (broad) halo. The sum of these components is shown as the full curve, and is shown to overlap the observed data. The difference between this calculated sum (i.e. the fitted curve) and the observed data is shown by the broken line oscillating around the baseline.

crystallizes in the γ form, and is similar to that observed in N6 except for the shortened chain-axis repeat. This shorter chain-axis repeat suggests that the 2_1 helix of the copolymer is less tightly coiled than in N6. The chain-axis repeat of

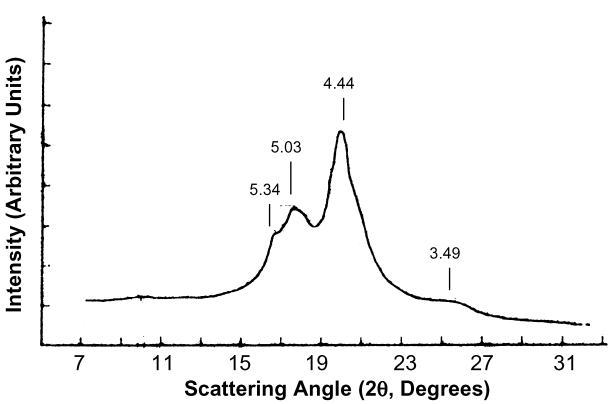

Fig. 10. XRD scan of 50:50 N6/AMCC powder (from Ref. [7]).

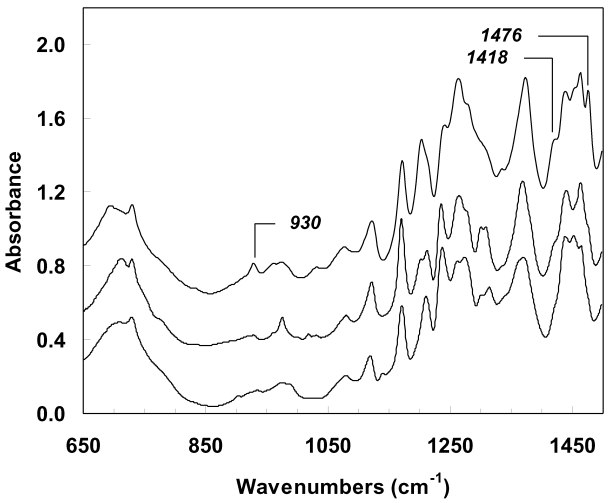

Fig. 11. Infrared spectra in the fingerprint region of the copolymer (17% AMCC) (bottom spectrum), nylon 6 γ (middle) and nylon 6 α (top) fibers.

15.7 Å in the copolymer represents the shortest ever helical pitch observed for N6: this distance in the α, γ, and iodine-complexes are 17.2, 16.9 Å, and 15.8 − 16.0 Å, respectively [18]. The shortened helical pitch is accompanied by an expansion of the lattice in the equatorial plane as seen in the data in Fig. 8 that show a shift in the equatorial peaks to

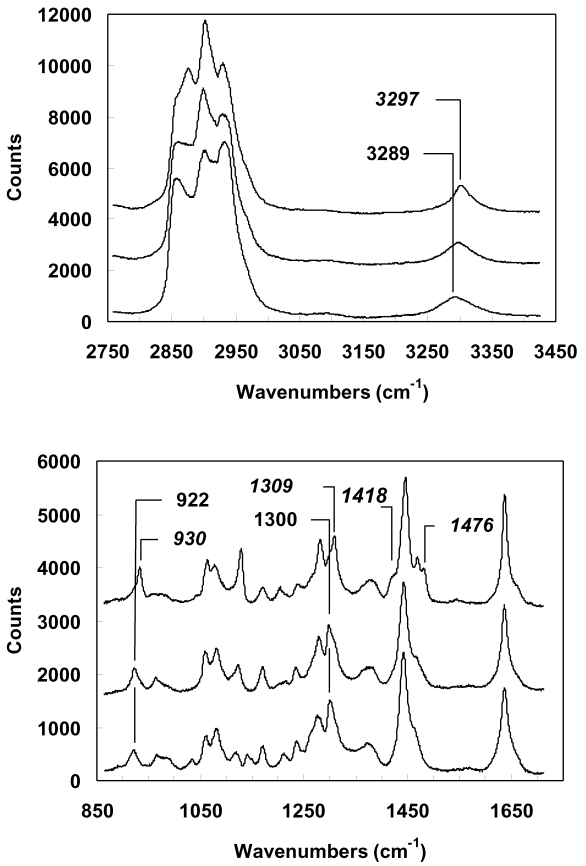

Fig. 12. Raman spectra of the copolymer (bottom spectrum), nylon 6 γ (middle) and nylon 6 α (top) fibers. Top panel shows the C–H/N–H stretch region and the bottom panel shows the fingerprint region.

lower angles. Typically, the γ crystals show an equatorial peak at $2\theta = 21.5°$ (0 0 1) and some times a second weaker peak or a shoulder at 22.7° (2 0 0 + 2 0 $\bar{1}$). The single equatorial peak seen in the copolymer is at 21.2° (Fig. 8a, c and 9). Whereas the γ form in the homopolymer transforms into α to varying degrees depending on the initial state of the γ crystals, e.g. it is easily transformed when the crystals have numerous defects/large microstrain, the γ in the copolymer was stable and remained unchanged even after autoclaving. In N6, the γ crystals are formed during rapid crystallization, and is thus of kinetic origin. In the copolymer, however, the γ form occurs because of chain-packing considerations, and is the thermodynamically stable crystalline form. Between 10 and 30 mol% of AMCC, the copolymer crystallizes in the γ-form indicating insertion of AMCC into the N6 crystal lattice. On the basis of the data presented by Prince et al., [7] we speculate that above 30%, the copolymer crystallizes in a new lattice that resembles that of AMCC, and at 50%, the copolymer lattice is almost the same as that of AMCC.

The large difference in the helical pitch of the copolymer and N6 clearly shows that AMCC segments were incorporated into the N6 lattice. But, this is not cocrystallization, i.e. dissolution of AMCC residues in the N6 lattice or the side-by-side crystallization of the two phases. The resulting structure was similar to that of the γ from of the homopolymer. Because the T_g of the copolymer was quite different from that of N6, it is also clear that AMCC resides in the amorphous region as well. Furthermore, while in other copolymers of N6, the T_m goes through a minimum in the melting point as the concentration of the comonomer is increased, we find no such minimum. These findings support the previous characterization of this copolymer as resulting from isomorphous replacement of N6 unit by AMCC [6]. Because the lattice dimensions of the copolymer is different from that of N6, strictly speaking, the copolymer is crystallographically not a result of isomorphous substitution.

The γ form observed in our data is substantiated by the modeling calculation carried out using Polygraf [19]. The calculations suggest that energy is lowered by about 0.8 kcal/mol if the cyclohexane ring in one hydrogen-bonded sheet of the γ structure fits into the amide pocket of the adjacent hydrogen-bonded sheet. Such conformational constraints can explain the shortening of the helical pitch from 16.9 Å in the γ-N6 to 15.7 Å, and the concomitant increase in the lateral spacing in the copolymer. Previous work has shown that the N–H stretch frequency ($\sim 3290\ cm^{-1}$) is higher in the α crystalline form than in the γ, the chain-axis repeats of which are 17.2 and 16.9 Å, respectively [20]. The present observation of still lower N–H stretch frequency (Fig. 12) is consistent with the lowest observed helical pitch of 15.7 Å. We speculate that the H-bonds are stronger in the N6/AMCC copolymer than in the α and γ crystalline forms of the N6 homopolymer. The N–H stretch frequency, which is an indirect measure of the strength of the H-bond, correlates with the chain-axis repeat unit measured from X-ray data (Fig. 13). Coincidentally, the N–H stretch frequency also correlates with the chain-modulus of the α and γ forms of N6, and the copolymer (see below). The decrease in N–H stretch frequency is interpreted as a lowering of the N–H force constant due to the increased H-bonding with the amide carbonyls in adjacent chains.

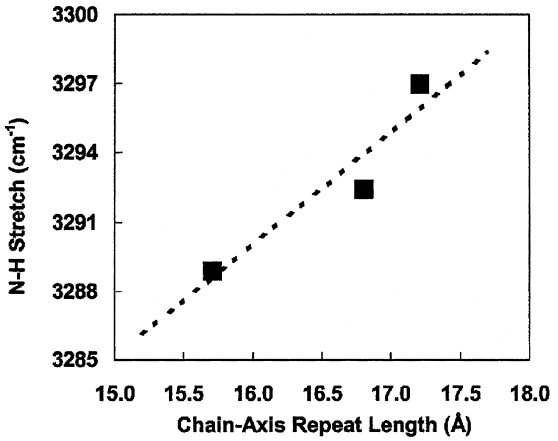

Fig. 13. Correlation between the N–H stretch frequency and chain-axis repeat unit for the three types of nylons.

The T_g of the copolymer is higher than that of N6 by about 25 °C indicating that the copolymer is stiffer than N6. But the theoretical modulus of the copolymer (93 GPa) [19] is only 30% of the fully extended α-N6 (295 GPa). This inconsistency can be reconciled if we note that the T_g-based stiffness arises from the mobility of the segments at large length scales (>10 Å), and is influenced by H-bonding. These H-bonds, some of which have to break at T_g and reform, are stronger in the copolymer. On the other hand, the theoretical modulus is determined by the structure at smaller length scale (<10 Å), and at these length scales the twisted chain conformation of the copolymer (helical pitch far less than that of N6) reduces the modulus of the fiber. This is consistent with the reduction in modulus of the γ form of N6 (135 GPa) [21] which is 45% that of the α form; the chain-axis repeat of γ is 16.9 Å and that of α is 17.2 Å. In addition to these two measures of stiffness, we have to consider a third one, the one that is reflected in the polymer

Table 4
Characteristics of textured yarns of N6 and the copolymer derived from detailed analysis of fiber diffraction data

Parameter	N6	Copolymer
Crystalline index (%)	52	30
α/γ ratio	76/24	0/100
Degree of orientation 0 2 0	0.902	0.931
Crystallite size (Å)		
Meridional 0 2 0—γ	60	
Equatorial 2 0 0—α	70	
Equatorial 0 0 2 + 2 0 2—α	40	
Equatorial 0 0 1—γ		95
Chain-axis repeat (Å)	17.1	15.7

modulus measured in mechanical testing apparatus. This modulus is determined by the stiffness of structures at larger length scales (~100 Å), the lamellar morphology of semicrystalline polymers [22,23]. The role of the amorphous regions becomes significant at these length scales, and will be discussed in Section 4.3.

The data in Tables 3 and 4 indicate that the crystallinity of the copolymer is about the same as that of N6 in as-cast films, but increases by a smaller amount than in N6 during annealing, and by an even smaller amount during drawing. Thus, in general, crystallinity of the copolymer is lower than that of N6 because the AMCC units hinder the crystallization of nylon. But this difference occurs during secondary crystallization, and even more so during orientation induced crystallization. Despite the lower crystallinity, and the lower chain-modulus, the modulus is the same in the two fibers (Table 1). It could be that stronger H-bonds increase the contribution of the amorphous domains to the fiber modulus.

4.2. Thermal characteristics

The melting temperature (T_m) of the copolymer extrapolated to 0% AMCC is the same as that for γ-N6. The T_m of the copolymer increases almost linearly with the increase in the AMCC fraction (Fig. 2c). This is different from that typically observed in other copolymers of N6 in which there is a minimum in T_m at some intermediate concentrations [4, 24]. Such a minimum would have indicated a eutectic and the formation of separate crystalline domains of each of the comonomers. Absence of this minimum in Fig. 2c suggests that we have a single crystalline phase, and this could be loosely construed as resulting from isomorphous replacement of AMCC units into the N6 lattice [6]. XRD and IR data show that this single phase of the copolymers is the γ form. The appropriate melting point for 0% AMCC is thus 214 °C corresponding to the γ crystals. Furthermore, data show that even small amounts of AMCC (as low as 5% that we have analyzed) drives the lattice into a single γ crystalline phase. The 222 °C melting point typically reported for N6 corresponds to the melting of α crystals of N6, a phase not observed in copolymers. A melting point of 222 °C for the 0% AMCC was erroneously used in an earlier paper to suggest that there is a eutectic at 5–15% AMCC concentration and that cocrystallization occurs in the copolymer [7].

This difference in the melting behavior of the copolymer and N6 is reflected in the crystallization behavior upon cooling. The copolymer crystallizes at a higher temperature than N6 (Fig. 3). This is to be expected because the copolymer crystallizes in the γ form, and N6 in the α (or predominately α) form. The γ form is kinetically favored in N6 but is thermodynamically stable in the copolymer; α is the thermodynamically stable form in N6.

Both T_g and T_{cc} increase linearly with the comonomer content suggesting that the comonomer affects the mobility of the chains in the amorphous regions in what appears to be a linear relationship. When the AMCC fraction exceeds 30%, the structure changes from a N6 lattice into an AMCC lattice, and the melting point suddenly increases to 355 °C. AMCC melts at 410 °C, has a T_g of 192 °C and crystallizes at 240–250 °C. Note, however, that despite the sudden increase in the T_m, there was a gradual increase in the T_g. This is to be expected as the T_m is determined by crystal packing considerations and the T_g is determined by the mobility of the polymer chains in the amorphous regions.

4.3. Effect of moisture

As can be seen from the data in Table 2, moisture has a marked effect on nylons, and AMCC substantially modifies the effect of moisture in the copolymer. We will attempt to understand this by examining structural changes at three length scales upon insertion of AMCC: the stiffness of the polymer chain due to an AMCC segment (length scale ~10 Å), stronger H-bonds between the chains (length scale >10 Å), and lower crystallinity of the copolymer (length scales ~100 Å).

At 51% RH, the T_g of the copolymer decreased by 62 °C from the corresponding dry-T_g and that in the homopolymer by a smaller amount of 52 °C. Higher T_g in the dry copolymer can be attributed to the stiff polymer chains and to the stronger H-bonds between the chains. These H-bonds enhance the local order and the stiffness of the amorphous segments of the copolymer when dry. Moisture interferes with the inter-chain hydrogen bonding, affects chain-mobility and hence the T_g. The H-bonds are now formed between the water molecules and the polymer chains making the amorphous segments considerably more mobile. A higher fraction of the amorphous phase in the copolymer combined with preexisting stronger interchain H-bonds, enables moisture to enhance the mobility to a greater degree in the copolymer than in N6. The stronger H-bonds (higher enthalpy) can also explain the higher T_m (by about 13 °C) of the copolymer over that of N6 when the samples were dry. On the other hand, in the presence of water, the T_m of the copolymer is 23 °C lower than that of N6 suggesting that the moisture weakens this H-bond effect and the contribution of the H-bond to enthalpy to a greater degree in the copolymer than in N6. This is consistent with larger decrease in T_g in the copolymer due to moisture.

The shrinkage measured in a fiber during unconstrained annealing at elevated temperatures was slightly smaller in the copolymer than in N6 when dry, but was almost twice that of N6 when wet. Local orientational order of the interfibrillar amorphous segments and the associated orientation of the crystals (length scales ~100 Å) are known to determine the amount of shrinkage [14]. Similar values of dry shrinkage in the two polymers suggests that the degree of amorphous orientation in the starting fibers, and the extent of loss of this orientation after exposure to heat, is about the same in the two fibers. This is to be

expected from rather similar processing conditions of the two fibers. Crystallinity differences are not expected to play a role in dry-shrinkage [14]. But in the presence of moisture, a larger fraction of the amorphous segments in the copolymer (lower crystallinity in the copolymer) accompanied by differences in H-bond strength and chain stiffness (differences in mobility), might produce the observed larger shrinkage in the copolymer than in N6. The same explanation can be used to account for the 33% larger creep elongation in the copolymer at 58% RH although dry-creep elongation were about the same in the two fibers.

Because the effect of water is greater in and causes the copolymer to shrink more, it would appear that moisture would also bring about a larger reduction in the modulus of the copolymer as well. But the data show that the modulus of films of the copolymer and N6 are similar at all levels of humidity (Fig. 4). This could be because of shrinkage is a consequence of reorientation of the crystals in the amorphous phase. Increased mobility of the amorphous chain segments over length scales of several monomer-lengths (>10 Å) due to the presence of water in the amorphous phase appears to accentuate this process to different degrees in the copolymer and N6. In contrast, modulus depends on the transfer of load from one chain segment to another, or from one crystallite to another through tie chains. This occurs over shorter length scales (~ 10 Å), for instance in the interlamellar regions. Moisture seems to have no differential effect on this aspect in the copolymer and N6, and thus the modulus decreases equally in both the copolymer and N6.

5. Conclusions

AMCC is incorporated into the N6 lattice (up to 30% AMCC substitution) forcing it to adopt the otherwise thermodynamically less favored γ conformation. The chain-axis repeat or the helical pitch in this γ structure is 15.7 Å, the shortest reported for N6, including that observed in iodine–N6 complexes. This reduces the modulus of the polymer chain relative to that of the α or the normal γ conformation. The higher T_g of the copolymer of N6 and AMCC when dry is attributed to stronger H-bonds that decrease the mobility of the polymer chain segments in the amorphous phase. The effect of water on the local order in the amorphous regions outside the lamellar stack is used to explain the larger decrease in T_g, and the larger heat-induced shrinkage of the copolymer in the presence of water. Changes in some of the properties induced by moisture make this copolymer attractive over N6 for certain applications.

Acknowledgements

We thank Dr R.S. Cooke who provided the samples used in this study, generously supplied with thermal and mechanical data that are discussed in this report, and offered constructive comments on the manuscript. The creep experiments were performed by Dr C. E. Osuch. We also thank Prof. P.H. Geil for his generous and helpful suggestions in the interpretation of the data. This work was supported in part by NSF EPSCOR grant EPS-0236976.

References

[1] Sonnerskog S. Acta Chem Scand 1956;10:113.
[2] Murthy NS, Wang Z-G, Akkapeddi MK, Hsiao BS. Polymer 2002;43:4905.
[3] Allegra G, Meille SV, Porzio W. In: Brandrup J, Immergut EH, editors. Polymer handbook. NewYork: Wiley; 1989. p. VI/339–46.
[4] Allegra G, Bassi IW. Adv Polym Sci 1969;6:549.
[5] Tranter TC. J Polym Sci Part A 1969;2:4289.
[6] Levine M, Temin SC. J Polym Sci 1961;49:241.
[7] Prince FR, Pearce EM, Fredericks RJ. J Polym Sci Part A-1 1970;8:3533.
[8] Xenopoulos A, Clark ES. In: Kohan MI, editor. Nylon plastics handbook. New York: Hanser; 1995. p. 107–37.
[9] Auriemma F, Petraccone V, Parravicini L, Corradini P. Macromolecules 1997;30:7554.
[10] Murthy NS. Polym Commun 1991;32:301.
[11] Atkins EDT, Hill MJ, Veluraja K. Polymer 1995;36:35.
[12] Murthy NS, Minor H. Polym Commun 1991;32:297.
[13] Sibilia JP, Murthy NS, Gabriel MK, McDonnell ME, Bray RG, Curran SA. In: Kohan MI, editor. Nylon plastics handbook. New York: Hanser; 1995. p. 69–106.
[14] Murthy NS, Bray RG, Correale ST, Moore RAF. Polymer 1995;36:3863.
[15] Murthy NS, Barton JrR. In: Chung FH, Smith DK, editors. Industrial application of X-ray diffraction. New York: Marcel Dekker; 2000. p. 495–509.
[16] Guinier A. X-ray diffraction. San Francisco: Freeman; 1963. p. 124.
[17] Arimoto H, Ishibashi M, Hirai M, Chatani YJ. Polym Sci Part A 1965;3:317.
[18] Murthy NS. Macromolecules 1987;20:309.
[19] Li Y, Goddard III WA, Murthy NS. Macromolecules 2003;36:900.
[20] Murthy NS, Stamm M, Sibilia JP, Krimm S. Macromolecules 1989;22:1261.
[21] Li Y, Goddard III WA. Macromolecules 2002;35:8440.
[22] Murthy NS, Grubb DT. J Polym Sci Polym Phys 2002;40:691.
[23] Murthy NS, Grubb DT. J Polym Sci Polym 2003;41:1538.
[24] Khanna YP, Murthy NS, Kuhn WP, Day ED. Polym Engng Sci 1999;39:2222.